Use of the Ultrasonic Through Thickness Test in Determining the Out-of-Plane Values of Stiffness Coefficients of SMCR26 Composites

Maina Maringa

Department of Mechanical Engineering, Jomo Kenyatta University of Agriculture and Technology, P. O. Box 62000, Nairobi, KENYA Email: maina_wamaringa@yahoo.com

ABSTRACT

Through thickness ultrasonic testing was carried out on specimens, which were cut out from Sheet Moulding Compound (SMCR26) sheets that had been obtained from the factory already moulded, with 26% by weight of randomly (R) oriented reinforcing short glass fibre, thus the acronym (SMCR26). This was done in order to determine the values of stiffness coefficients in the out-of-plane direction and to identify the presence or absence of any spatial trends, as well as that of transverse isotropy, the last feature, which is prevalent in most short fibre reinforced composites. The values of stiffness coefficients obtained were all lower in magnitude than the known in-plane values of elastic modulus, which from the definition of stiffness coefficients implied that the out-of-plane values of stiffness were less in magnitude than the in-plane values. The lower values were also consistent with expectations stemming from the formulation process for the SMCR26 sheets, which tended to align the reinforcing fibre along the in-plane axes and not in the out-of-plane axis. The values of stiffness coefficient obtained were also seen to vary from point to point, signifying that the material is heterogeneous.

***KEY WORDS*:** Ultrasonic, Sheet Moulding Compound (SMCR26), Stiffness Coefficients

1.0 NOMENCLATURE

D	Distance or path length
λ	Wavelength
l	Characteristic length
T	Time
ΔT	Time difference
ρ	Density

C_{ij}	Stiffness coefficient
E	Elastic modulus
λ_L	Lame's constant
μ	Shear modulus
v_l	Compression wave velocity
c	Speed or velocity
v_t	Shear wave velocity
ν	Poisson's ratio
KHz	Kilo Hertz
GPa	Giga Pascal
Mpa	Mega Pascal
KPa	Kilo Pascal
xx, yy, zz	Cartersian Co-ordinate directions
11, 22, 33	Cartersian Co-ordinate directions

2.0 INTRODUCTION

Sheet moulding compound is formulated using short reinforcing glass fibre that are scattered onto a moving sheet of compounded polyester limestone filler matrix and the mixture subsequently needled with needling rollers with the aim of giving it a two-dimensional planar random fibre distribution and therefore, transverse isotropy. Uniaxial tensile tests conducted elsewhere (Maringa, 2002), indicated the presence of directional and spatial variations in the values of stiffness and strength for the SMCR26 that was used here. However, because of the small number of test specimens used, 15 and 12 in to mutually orthogonal directions, it was necessary that further testing be carried out to verify this observation. Noting that the tensile test was destructive and that the available stock of SMCR26 sheets was very limited, it was deemed necessary to adopt non-destructive methods for further testing. The small amplitude transverse vibration test was adopted for use in the determination of the in plane values of stiffness, while the ultrasonic through thickness test was chosen for use in the determination of the out-of-plane values of stiffness and stiffness coefficients, respectively, for the SMCR26 sheets, in that order. Unlike the case for the tensile and small amplitude transverse and longitudinal vibration tests, the small thickness of the SMCR26 sheets, 3mm, was not a constraint for the ultrasonic through thickness method. The ultrasonic through thickness test also offered the added advantage of being easy to execute and facilitated the rapid acquisition of large amounts of data. The results of small amplitude transverse vibration testing of SMCR26 confirmed the directional and spatial dependency in the properties

stiffness of the material (Maringa, 2002). In addition to providing the out-of-plane values of stiffness coefficients for SMCR26, comparison of the spatial distribution and directional dependency of the through thickness ultrasonic test results and those obtained from the small amplitude transverse vibration test, were expected to confirm the presence or absence of transverse isotropy.

2.1 Sheet Moulding Compound

Short fibre reinforced composites fall into the three categories of aligned discontinuous, off-axis discontinuous and randomly oriented discontinuous fibre reinforced composites. This last type is the most widely used, due to the ability of short fibres to mix easily with liquid resins, thus facilitating quick and low cost production of complex component geometry, by injection moulding or compression moulding processes (Gibson, 1994).

Sheet moulding compound (SMC), is one of a number of polyester moulding compounds including, dough moulding compound (DMC), also known as bulk moulding compound (BMC), chopped strand mat (CSM), woven roving (WR) and polyester resin reinforced with unidirectional (UD) reinforcing fibres (Johnson, 1992). Polyester moulding compounds are composed mainly of polyester resin, limestone filler and reinforcing glass fibre, with minor additives such as low profile additives (LPA's), inhibitors, and thickeners, as well as mould release agents and pigments. Sheet moulding compound finds application mainly in the production of car body panels and fenders, partition walls, furniture, as well as casings for electronic and household goods.

Limestone filler is normally added into the polyester resin matrix in order to increase its bulk and to improve handling of the matrix. Glass fibre of between 20 – 50 mm in length and with weight fractions of 20%, 25%, 30% or 35%, is in turn added to the polyester resin/limestone filler base in order to increase its strength (Garroch, 1996). While the maximum possible volume fraction for square and hexagonal close packed longitudinally aligned continuous reinforcing fibres is 78.5% and 90.7%, respectively, the actual values for SMCR are limited by the need to maintain good rheological properties to between 25 – 50% (Hull and Clythe, 1996).

During formulation of SMCR26, chopped glass fibre is first dropped freely onto a layer of the polyester/limestone matrix that is carried on a moving thin film of polyethylene. The composite is then needled with needling rollers in order to ensure proper wetting and 2-dimensional planar random distribution of the reinforcing glass fibre. Though the resulting composite is normally assumed to be macroscopically isotropic and homogenous, the needling process is likely to introduce directional properties to the resulting composite (Maringa, 2002). After needling, the SMC sheets are then left to cure for periods that can be reduced to between 2-3 days with the addition of thickeners and then cut up into various required sizes for storage. Subsequent hot or cold press moulding into a final required component shape, before cure of the SMC material, in which the mould charge is normally limited to between 90–100% of the mould charge area (Garroch, 1996), is likely to introduce or enhance directionality of the product. Hot press moulding is carried out at pressures and temperatures of 1 MPa and 100 – 130 °C, respectively, for normal charges, and at pressures and temperatures of 1–7 MPa and 120 – 170 °C, respectively, for moulding compounds with additives that increase the charge viscosity. Cold press moulding on the other hand is carried out at room temperature and at a pressure of 120 KPa, with a typical cycle time of about 5 minutes (Birley, 1992; Johnson, 1992, 1986; Bowen, 1992; Melby and Castro, 1989; Whelan and Goff, 1989). Typical values of stiffness for SMC are given in Table 1 below, after the work of Johnson (1992).

Table 1 Typical Values of Some Mechanical Properties of SMC

Property description.	Statistical measure	Statistical value
Glass fibre content (%)	Average	30
	Range	20 – 40
Tensile stiffness (GPa.)	Average	13
	Range	11 - 16
Flexural stiffness (GPa.)	Average	11
	Range	7 - 14

2.2 Ultrasonic Through Thickness Testing

Sound waves are categorised as a function of their frequency range into infrasonic waves (0 – 16 Hz), sonic hear waves (16 Hz –20 kHz) and ultrasonic waves (>20 kHz). Sound waves are transmitted by a simple knock on effect in which the energy in a particle vibrating about an equilibrium position is passed on to adjacent particles. For longitudinal waves (also referred to as compression waves), this creates areas of rarefaction and compression in the transmission media or materials, (Hinsley, 1959). Both longitudinal waves and shear waves (also known as transverse waves), are propagated in solid media, while liquid media only support the propagation of the longitudinal waves, which in this case are referred to as bulk waves (Hinsley, 1959; Halmshaw, 1991; Shutilov, 1988; Rose, 1999). Elliptical free waves, also referred to as surface or Rayleigh waves, plane strain or Lamb waves and free or Love waves are some other category of ultrasonic waves that are also defined by their manner of propagation (Halmshaw, 1991; Rose, 1999; Shutilov, 1988). Detailed derivations leading to the following two general expressions for the longitudinal and transverse wave velocities of sound waves propagating in solid media away from the boundaries of the propagating media are to be found in the separate works of Stumpf (1980), Shutilov (1988) and Rose (1999): -

$$v_l = \sqrt{\frac{(\lambda_L + \mu)}{\rho}} = \sqrt{\left(\frac{E}{\rho}\right)\frac{(1-\nu)}{(1+\nu)(1-2\nu)}} \quad \text{1a}$$

$$v_t = \sqrt{\frac{\mu}{\rho}} = \sqrt{\left(\frac{E}{\rho}\right)\frac{1}{2(1+\nu)}} \quad \text{1b}$$

Ignoring the Poisson's ratio in these two expressions reduces them to the following two more commonly known expressions for the propagation of ultrasonic waves in solid media, which give good first estimates of any required parameters.

$$v_l = \sqrt{\frac{(\lambda_L + \mu)}{\rho}} = \sqrt{\left(\frac{E}{\rho}\right)} \quad \text{2a}$$

$$v_t = \sqrt{\frac{\mu}{\rho}} = \sqrt{\left(\frac{E}{2\rho}\right)} \quad \text{2b}$$

The interested reader is referred to the separate works of Van Buskirk et al (1986), Rose et al (1990), Rose et al (1991) and Khoury *et al* (1999), which contain

detailed mathematical derivations describing the propagation of ultrasonic waves in solid media and their use in determining the stiffness coefficients of various types of materials.

Ultrasonic non-destructive testing methods trace back to their early description by Sokolov in 1935 and application by Firestone in 1940 respectively (Michael Berke, 2001). Ultrasonic transducers today find application in a wide variety of areas such as flaw detection, measurement of thickness and characterisation of materials using bulk waves in (Frielinghaus, 2001) tube-inspection using and guided waves (Hackenberger and Rose, 1998). Piezocomposite transducers with their broad band, short pulse duration waves and high pulse amplitudes are preferable to PZT and PVDF transducers for use on materials with high attenuation characteristics such as composites, plastics, cast iron and austenitic steel (Splitt, 2001). Ultrasonic phased array technology, which has been available for medical use and for the inspection of welded steel tubing since the 1970's, is now available for other industrial applications as a result of the increased sensitivity of electronic devices and availability of advanced computer systems (Standards Steel, 2001). Phased arrays typically have up to 256 elements, with element sizes as small as 0.5 mm and inter-element gaps of 0.03 mm. The respective array probes can be used to generate angled, focused or linear travelling ultrasonic wave beams, by manipulating the order in which the elements in an array are fired. This facilitates the inspection of complex component shapes and the targeting of specific areas of importance (Lonsdale and Meyer, 2000).

Signal attenuation of ultrasonic waves occurs in two forms, namely scattering and absorption. The former occurs as a result of the abrupt change in wave velocity as an ultrasonic wave travels through materials with varying impedances as a result of the presence of in-homogeneities existing in materials. In-homogeneities occur in materials in the form of crystals with different orientations and different mechanical properties in their different directions and also in the form of gas pores and flaws in a material. In-homogeneities also arise from the use of different elements with different properties in the production of alloys and composites and also due to the presence of different sizes of grains in a material. In the case where the wavelength of the propagated wave is of the same order as the encountered in-homogeneity, the propagated wave is split at the boundaries of the in-homogeneity into refracted and reflected components, in what is

referred to as geometric division. This for a high number of in-homogeneities may generate a lot of noise, normally referred to a "grass" that could in certain cases even overshadow the main signal, making it impossible to detect. In cases where the wavelength of the transmitted wave is much bigger than the in-homogeneities, scatter will occur in the same manner as that of a light wave split up by the presence of small water droplets. Signal attenuation may also occur through the absorption of energy from the transmitted wave by the medium of propagation, which is then converted into heat energy. This form of attenuation increases in significance with the increasing frequency of the propagated wave (KrautKrämer et al, 1990).

It is important to ensure that the wavelength (λ) of the incident wave is much greater than the nominal dimensions (l) of any encountered heterogeneity, for heterogeneous materials, in order to minimise scatter and absorption of the incident ultrasonic beam and the accompanying attenuation and/or loss of signal. A factor of $\lambda/l \geq 10$ is normally used to this end (Gibson, 1994). Because of the fact that composites are composed of different materials with different properties, the elastic moduli for heterogeneous composites will vary from point to point. This is particularly so for randomly oriented, short fibre reinforced composites. The elastic moduli of such materials are therefore best represented as effective elastic moduli, through a smearing effect that averages the elastic moduli over representative volumes. This is achieved in ultrasonic testing by ensuring that the wavelengths of the propagated waves are much larger than the nominal size of discontinuities in the composite thus minimising scatter. The wave frequencies are also set much lower than the resonance frequencies of the constituents in order to minimise dispersion of the propagated waves (Gibson, 1994; Rose, 1999).

Poor contact between the ultrasonic probes, which are designated as transmitter and receiver, is another cause of signal attenuation, which is easily resolved using coupling agents such as: oil, glycerine, grease, silicon oil and soluble cellulose. Washing up liquid was found in the present work to be as effective a coupling agent as the normally recommended silicon oil/jelly, for SMCR, various types of limestone, aluminium and steel specimens that were tested in the present work. Washing up liquid has the added advantage as a couplant because of its better wetting properties

(KrautKrämer et al, 1990). Because of its lower cost and better availability, washing up liquid was therefore, adopted for use in the present work, in place of silicon gel. Though the corrosive effect of water on metallic surfaces can be reduced through addition of inhibitors such as trisodium phosphates to any couplants used (KrautKrämer et al, 1990), the use of washing up liquid in the testing of in-service metallic components or metallic specimens that require further use over a period of time, is not advisable as it is still likely to introduce corrosion.

When sound approaches an interface, it may be reflected entirely or transmitted and reflected simultaneously in different proportions, as a function of the relative velocities of transmission in the two interfacing media and its angle of incidence at the interface. Thus for a liquid/solid or gas/solid interface, the incident wave is reflected and refracted in its decomposed state of a compression and shear wave, at the interface with the shear wave refraction angle being greater than that for the compression wave. In the case of a solid/solid interface with an incident compression wave, the result is the same as for the previous case, with the additional fact that decomposition into compression and transverse waves occurs for the reflected wave as well (KrautKrämer et al, 1990; Hull and John, 1988; Halmshaw, 1991). In order to avoid creating confusion, the incident angle is normally set to angles greater than the first critical angle, at which the transmitted compression wave is fully internally refracted (Hull and John, 1988), thus becoming a compression surface wave and thus leaving the shear wave as the only transmitted wave. Thus for the Perspex /steel interface for instance, the first critical angle is 27.5^0 and angle probes for this system are normally available at 35^0, 45^0, 60^0, 70^0 and 80^0. By setting the incident angle to 57^0, which is the second critical angle for the perspex/steel system, the transmitted shear wave is totally internally refracted to produce surface Rayleigh waves.

The percentage energies of the transmitted (transimissivity E_T) and refracted (reflectivity E_R) components of a sound wave that is incident at an interface, have been presented separately by Kavishe (1997) and Halmshaw (1991) as a function of the acoustic impedances of the two interfacing media as:

$$E_R = \left[\frac{(Z_1 - Z_2)}{(Z_1 + Z_2)}\right]^2 \quad \text{..... 3a}$$

$$E_T = \frac{(4Z_1Z_2)}{(Z_1+Z_2)^2} \quad \text{3b}$$

By substituting the values of the acoustic impedances for the two materials in an air/steel and a water/steel interface, reflectivity values of 0.99 and 0.88 were given in the two separate works, respectively. The authors further showed that high values of reflectivity coincided with a low values of transmissivity and vice vasa. The low transmissivity of the air/steel interface is such as to demand a reduction in the percentage of the reflected energy. This is achieved by placing couplants in between the two media, which have higher values of impedance than air and which are normally fluids in order to ensure proper wetting of the surface that they are applied to (Kavishe, 1997; Hull and John, 1988; KrautKrämer et al, 1990). The effect of couplants, such as water and oil is to decrease the reflectivity, with a coincident increase in the transmissivity to values of about 94% and 96%, respectively (Hull and John, 1988). KrautKrämer et al, (1990) noted that the glycerine had the highest acoustic impedance of all chemically acceptable liquid couplants, with oil being the most widely used. They also observed that grease, petroleum jelly and a paste made from a mixture of water and methyl cellulose (wall paper paste) were all used as couplants for vertical or inclined surfaces, as their, relatively higher viscosities stopped them from flowing. The authors further noted that water at high velocities also served as a useful couplant at temperatures as high as 400^0 C.

3.0 EXPERIMENTATION

It must be noted here that since the SMCR26 sheets from which test specimens were obtained, were acquired from the factory already moulded, no information is given here on the moulding process for the material, rather the section focuses on dimensioning of the test specimens. As no standards are in force on the preparation of through thickness ultrasonic tests specimens, no standards have been quoted either.

Figures 1 and 2 below show the dimensions of the parent SMCR26 sheets and the sectors within the central charge area from which test specimens were obtained, respectively. In order to ensure consistency of directions, the longitudinal and transverse direction of the parent SMCR26 sheets were taken to be the longer and shorter direction, respectively.

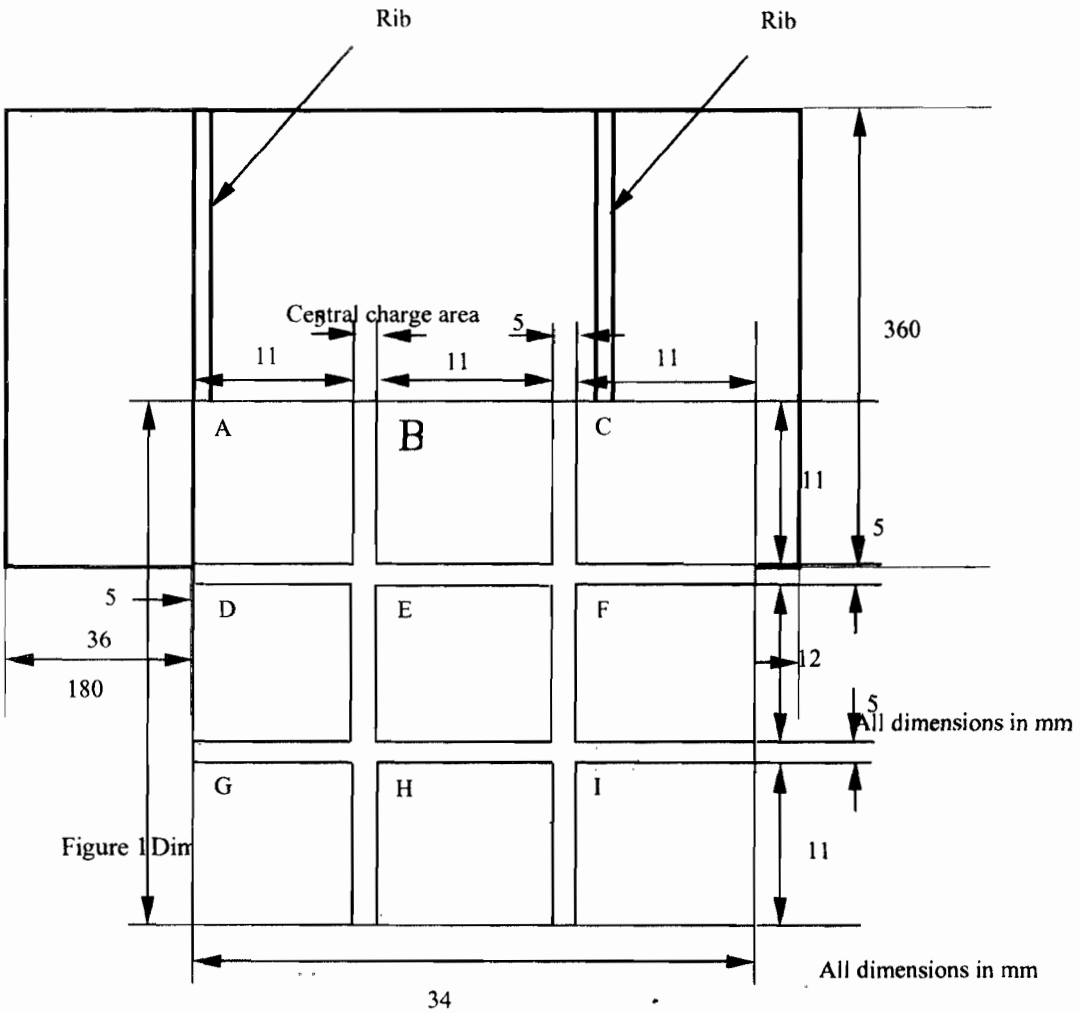

Figure 1 Dim

Figure 2. Location of the nine sectors within the central charge area from which specimen were obtained

The length of the specimens whose longitudinal directions were aligned parallel to and orthogonal to the longitudinal direction of the parent SMCR26 sheets was 120 mm and 115 mm, respectively, while the width and thickness of each specimen were 17.6 mm and 3mm, respectively. In addition to testing of the SMCR26 specimens, preliminary tests were conducted using aluminium specimens, as controls, in order to verify the accuracy of the data obtained from the ultrasonic testing-rig. Three specimens each of aluminium were used with nominal length, width and thickness dimension of 120 mm, 20 mm and 3 mm, respectively. Three measurements of each dimension were obtained and

averaged, for each specimen and their respective weights determined prior to ultrasonic testing, and the results recorded for latter use in determining the densities of each specimen.

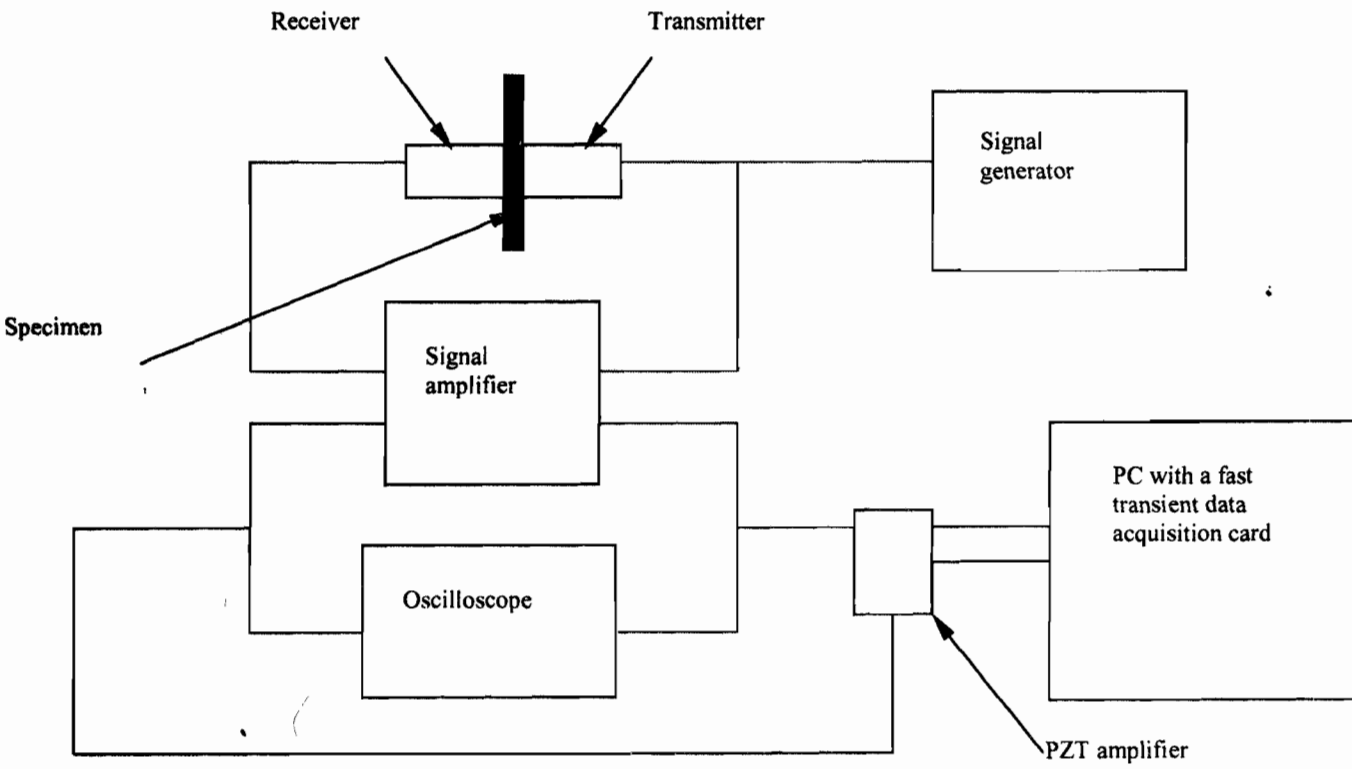

Figure 3 Layout of the ultrasonic through thickness tests equipment.

Through thickness tests were carried out at five different locations along the length of each SMCR26 specimen, using the equipment layout shown in Figure 3. For each set of readings, washing up liquid was applied to the specimen at the location to be scanned and then the transmitter and receiver probes fixed firmly, using a screw driven clamp, on opposite sides of the specimen at the selected location. An electric pulse was generated using the signal generator and injected into the transmitter, which in turn generated an ultrasonic signal that was then transmitted through the specimen thickness and into the receiver, thus generating an electric pulse in it.

The probes that were used in the present work were rated at 5 MHz and were cylindrical in shape with a diameter of about 27 mm. This of course limited the size of element that could be scanned at any one time and implied that the values of through thickness velocity obtained using them were averaged values for any one area scanned. The probes were made of an outer aluminium casing with a protective shoe on the contacting surface behind which was the piezoelectric sound generating transducer. Descriptive material and sketches on the construction of compressive and shear ultrasonic probes can be found in the text by Kavishe, (1997). More details of the different types of probes, including fixed and rotating angle probes, single and phased arrays, thickness gauges and flaw detectors can be obtained from the Panametrics and KrautKrämer web sites, http://www.panametrics-ndt.com/ and http://www.geinspectiontechnologies.com/products/Ultrasonics/

Profiles of the transmitted and received ultrasonic signals were simultaneously displayed on an oscilloscope, and the width and period of the generated input pulse varied in order to obtain acceptable signal profiles. The best profiles of the transmitted and received signals were obtained through trial for values of period, delay and width of the transmitted signal of 10 μs, 10 μs and 10 ns, respectively. A fast transient data acquisition card, installed in a 486 PC, was used to collect digitised data of time and amplitude of the generated and received signal pulses. The card was triggered using "TRANS8CH" software provided by the Experimental Office of the School of Engineering, at the University of Manchester. The software was also used to select and make the settings for the various channels that were used to collect data, thus determining the regularity of data collection and the time span over which data was collected. The software provided for the storage of acquired data in BDAT format, as well as in ASCII format spreadsheets. The data in the spreadsheets was stored in three columns of time, and amplitudes for the transmitted and received signals. Data analysis was subsequently done using a Matlab code named "USONICS", which was developed to handle the large amount of data collected (Maringa, 2002), which for the 99 SMCR26 specimens tested was stored in 2500 different data files. The two signals were also captured using a first transient data acquisition card and stored in a PC for latter analysis. On completion of testing each specimen was dried with cloth and kept aside for further testing if required.

4.0 RESULTS

4.1 Calibration And Zero Error Testing

Figure 4 shows sample traces of the generated and received signals for the case of a contacting transmitter and receiver, with the traces for the received signal in this figure, translated upwards by 0.2 units on the graphs in order to facilitate easy viewing of the labelled point. The labels A and B in the figures show the minimum points of the traces that were used to determine the travel time ΔT for propagated ultrasonic waves as $\Delta T = T_B - T_A$. The travel time thus determined was then used to calculate the velocity c of propagation of ultrasonic waves based on the equation $c = (D/\Delta T)$, where the symbol D stood for the path length, which was equal to the specimen thickness. Values of the stiffness coefficients C_{33} for the propagation media were then calculated using Equation 1a, $v_l = \sqrt{\left(\frac{E}{\rho}\right)\frac{(1-\nu)}{(1+\nu)(1-2\nu)}}$, for the propagation of longitudinal waves. A Poisson's ratio value of 0.33 [Kirkwood (1985)] was adopted for the aluminium specimens.

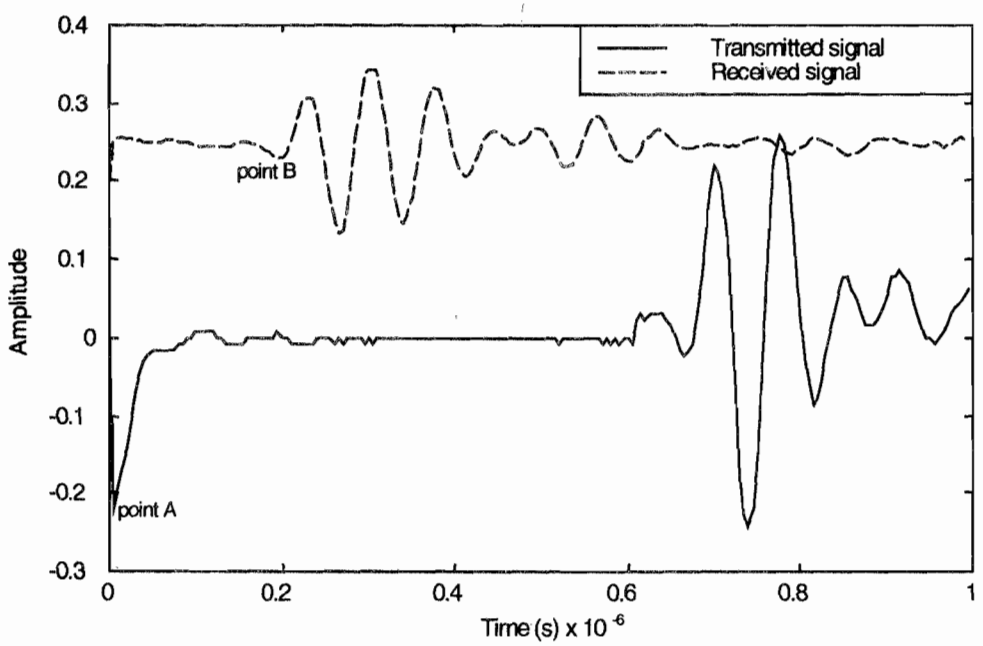

Figure 4 Typical generated and received ultrasonic signal traces for transmitter and receiver transducers that were in direct contact

The fact that the minimum points for the two traces in Figure 4 were not coincident clearly pointed to the presence of a zero error, which needed be subtracted from the values of transmission time measured for any test specimen. A contacting transmitter/receiver zero error transmission time correction (*zetr*) of 0.615 μs. was obtained by averaging the time difference between such two minimum points for 20 traces, each obtained from a separate contacting transmitter/receiver test run.

Figure 5 shows typical traces for the aluminium specimens that were tested, clearly exhibiting the minimum points for the transmitted and received ultrasonic signal curve traces.

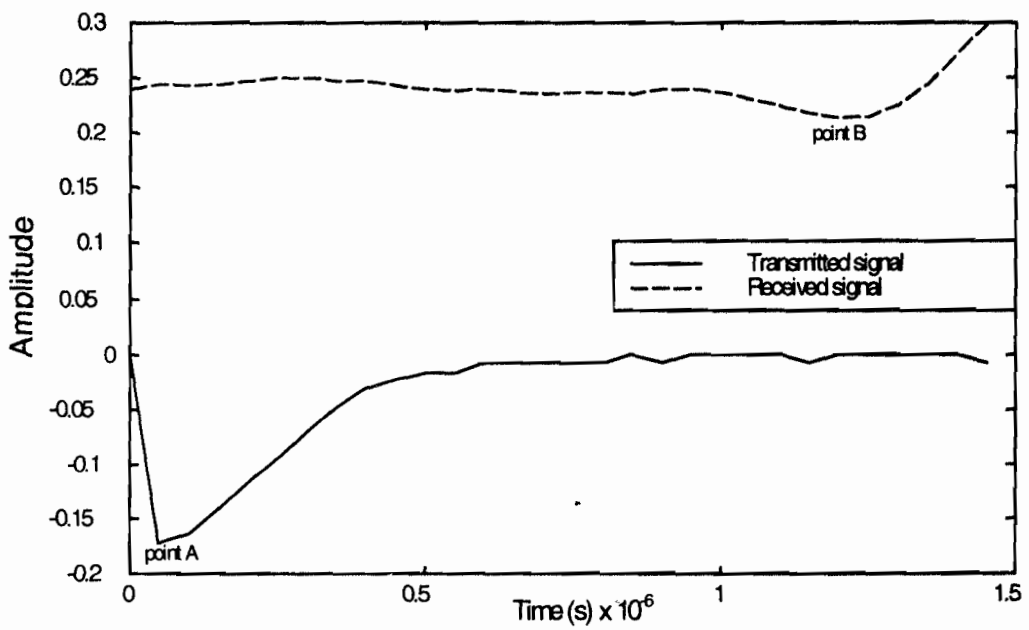

Figure 5 Typical generated and received ultrasonic signal traces for an aluminium specimen

The stiffness coefficient for aluminium can be easily shown to be equal to 78.55 GPa, from the known values of elastic modulus and Poisson's ratio of 70 GPa and of 0.33, respectively. Values of stiffness coefficients of 51.46 GPa, 47.95 GPa and 51.32 GPa for aluminium, were obtained however, from the ultrasonic test results based on the zero error transmission time correction *(zetr)*. The fact that the experimental values of stiffness

coefficient were much lower than the theoretical ones for aluminium was an indication that the zero error transmission time correction (*zetr*) for a single coupling liquid interface, was smaller than the one prevailing for two interfaces of coupling liquid. The zero error transmission time correction for the two interfaces of coupling liquid was adjusted therefore, until the experimental values of stiffness coefficients for the aluminium specimens were equal to the known value of 78.55 GPa. This was achieved for an average zero error transmission time correction (*zeal*) for the aluminium specimens of 0.728 μs.

Table 2 shows the values of stiffness coefficients that were obtained with this new value of zero error transmission time correction (*zeal*) as well as those that had been obtained with the zero error transmission time correction (*zetr*)

Table 2 Values of Stiffness coefficient C_{33} for isotropic aluminium specimens

Specimen number	1	2	3
C_{33} for zetr = 6.1500e-007s	51.46 (GPa)	47.95 (GPa)	51.32 (GPa)
C_{33} for zeal = 7.2800e-007s	81.05 (GPa)	73.84 (GPa)	80.73 (GPa)
Average for zetr = 6.1500e-007s	50.24 (GPa) – 36% less than the known value		
Average for zeal = 7.2800e-007s	78.54 (GPa) – 9.17 x 10^{-3}% less than the known value		

The error in the average value of stiffness coefficient C_{33} obtained using the zero error transmission time correction (*zeal*) is seen from this table to be considerably smaller than the error arising from use of the zero error transmission time correction (*zetr*). This justified use of the zero error transmission time correction (*zeal*) in preference to the zero error transmission time correction (*zetr*). The differences between the values of stiffness obtained using either one of these two corrections for SMCR26 however, are expected to be lower than those shown in Table 2 above, if the transmission velocity of ultrasonic waves through the material is lower than in aluminium. It must be pointed out however, that the coupling efficiency of various materials and surfaces is likely to differ, thus demanding use of correction factors that are specific to particular materials and coupling efficiencies. Maringa, (2002) showed the differences in the values of transmission time obtained from different locations of the same specimen of specific types of limestone for

different types of limestone to be negligibly small, which was an indication that this latter effect could be ignored.

4.2 Results for the SMCR26 specimens

Tables 3 and 4 show the average values of thickness and density for SMC specimens that were aligned parallel and orthogonal to the longitudinal sheet direction, respectively. The values of thickness and density in these tables are all averages of three separate measurements of the dimensions and weights for each specimen.

Table 3 Average values of thickness and density for SMCR26 specimens that were aligned parallel to the longitudinal sheet direction

	SECTOR A		SECTOR B		SECTOR C	
Specimen No.	Thickness (m)	Density × 10^3 (kg/m^3)	Thickness (m)	Density × 10^3 (kg/m^3)	Thickness (m)	Density × 10^3 (kg/m^3)
1	0.0031	2.3403	0.0032	2.3761	0.0032	2.3333
2	0.0031	2.3204	0.0032	2.3251	0.0033	2.3215
3	0.0031	2.2901	0.0032	2.3333	0.0033	2.3136
4	0.0031	2.2941	0.0032	2.3373	0.0033	2.2776
5	0.0031	2.3056	0.0032	2.3344	0.0033	2.2851
6	0.0031	2.2889	0.0031	2.3414	0.0032	2.2889
	SECTOR D		SECTOR E		SECTOR F	
1	0.0031	2.3305	0.0032	2.3178	0.0032	2.3116
2	0.0031	2.3156	0.0032	2.3172	0.0032	2.3275
3	0.0031	2.2850	0.0032	2.3140	0.0032	2.3206
4	0.0030	2.3329	0.0032	2.3088	0.0032	2.3218
5	0.0031	2.2555	0.0032	2.3081	0.0032	2.3030
6	0.0031	2.3068	0.0032	2.2892	0.0032	2.2819
	SECTOR G		SECTOR H		SECTOR I	
1	0.0031	2.2792	0.0031	2.3266	0.0032	2.3115
2	0.0030	2.3368	0.0031	2.2878	0.0032	2.3071
3	0.0030	2.3045	0.0030	2.3361	0.0031	2.3175
4	0.0030	2.2754	0.0030	2.3151	0.0032	2.3008
5	0.0030	2.2837	0.0030	2.3274	0.0031	2.3190
6	0.0030	2.2904	0.0030	2.3108	0.0031	2.2952

Table 4 Average values of thickness and density for SMCR26 specimens that were aligned orthogonal to the longitudinal sheet direction.

	SECTOR A		SECTOR B		SECTOR C	
Specimen No.	Thickness (m)	Density × 10^3 (kg/m^3)	Thickness (m)	Density × 10^3 (kg/m^3)	Thickness (m)	Density × 10^3 (kg/m^3)
1	0.0031	2.3393	0.0032	2.2833	0.0032	2.3318
2	0.0031	2.3348	0.0032	2.2664	0.0032	2.3048
3	0.0031	2.3288	0.0032	2.2833	0.0032	2.3220
4	0.0031	2.3322	0.0032	2.2709	0.0032	2.3042
5	0.0031	2.3266	0.0032	2.2777	0.0032	2.3128
	SECTOR D		SECTOR E		SECTOR F	
1	0.0031	2.2406	0.0032	2.2546	0.0032	2.2919
2	0.0032	2.2225	0.0032	2.2516	0.0032	2.2777
3	0.0031	2.2540	0.0032	2.2402	0.0032	2.3013
4	0.0031	2.2382	0.0032	2.2462	0.0032	2.2981
5	0.0031	2.2571	0.0032	2.2531	0.0032	2.2900
	SECTOR G		SECTOR H		SECTOR I	
1	0.0030	2.3067	0.0030	2.3081	0.0031	2.2917
2	0.0030	2.2714	0.0030	2.2992	0.0031	2.2684
3	0.0030	2.3126	0.0030	2.3000	0.0031	2.2635
4	0.0031	2.2255	0.0031	2.2647	0.0032	2.2101
5	0.0030	2.2562	0.0031	2.3112	0.0031	2.2664

The values of density given in these two tables were used together with the calculated values of longitudinal wave velocities for each location on every specimen, to calculate the values of stiffness coefficients for the zero error transmission time correction (*zeal*). A Poisson's ratio value of 0.285 (Garroch, 1996) was used to calculate the velocities of transmission of ultrasonic waves in the SMCR26 specimens. The values of longitudinal wave velocities, for each location on every SMCR26 specimen, were determined as the average of five different values each obtained from curves such as the one shown in Fig. 6.

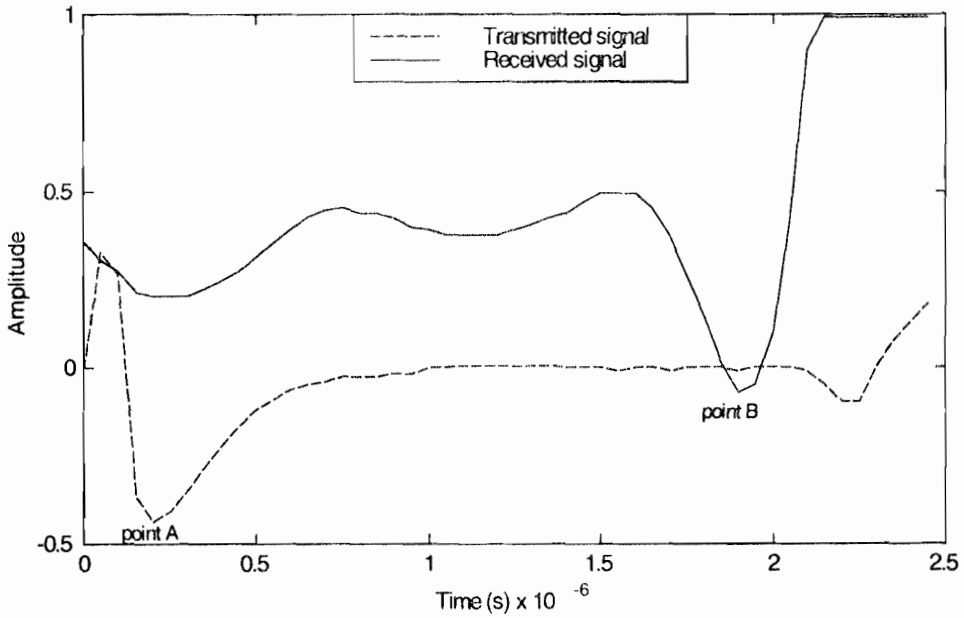

Figure 6 **Typical generated and received ultrasonic signal traces for a SMCR26 specimen**

Tables 5 and 6 give the values of stiffness coefficients based on the zero error transmission time correction (*zetr*), calculated by substituting the average of five values of longitudinal velocities, determined at each location on every SMCR26, into Equation 1a.

Table 5 **Stiffness coefficients C_{33} for SMCR26 specimens that were aligned parallel to the longitudinal parent sheet direction.**

	SECTOR A	SECTOR B	SECTOR C
Specimen no.	C_{33} (GPa)	C_{33} (GPa)	C_{33} (GPa)
1	10.4184	10.4912	9.9656
2	10.4131	11.7758	9.5108
3	10.2632	10.3029	9.4216
4	10.3240	10.6051	9.2502
5	10.1975	9.7620	9.2216
	SECTOR D	SECTOR E	SECTOR F
1	10.3947	9.5965	9.1655
2	9.8689	9.6555	9.2574
3	10.0350	10.9833	9.0031
4	10.3380	9.6543	9.1107
5	9.8324	10.2557	8.9745
	SECTOR G	SECTOR H	SECTOR I
1	9.6783	10.6360	10.1496
2	9.9185	10.3116	10.0855
3	10.2050	9.9291	10.9426
4	10.2424	9.5909	10.7637
5	10.8301	9.5338	10.9634

Table 6 Stiffness coefficients C_{33} for SMCR26 specimens that were aligned orthogonal to the transverse parent sheet direction.

	SECTOR A	SECTOR B	SECTOR C
Specimen no.	C_{33} (GPa)	C_{33} (GPa)	C_{33} (GPa)
1	13.2405	9.1619	9.7966
2	12.8367	9.1770	9.5489
3	12.5401	9.2278	9.1606
4	11.9163	8.8128	8.4288
5	11.7239	8.7578	8.6372
	SECTOR D	SECTOR E	SECTOR F
1	9.6822	9.6233	9.5114
2	9.3623	9.4311	9.3905
3	9.6457	9.6003	9.2322
4	10.3995	9.9199	8.8792
5	9.9366	10.3136	8.8339
	SECTOR G	SECTOR H	SECTOR I
1	9.8136	12.0580	9.4352
2	9.6903	11.3158	9.1675
3	10.2051	10.9952	9.0826
4	10.9606	10.3867	9.1466
5	10.3419	10.3714	9.0435

5.0 ANALYSIS AND DISCUSSION

The values of stiffness coefficients given in Tables 5 and 6 are presented graphically in Figures 7 (a and b), in order to give a proper idea of their variation over the surface of the parent SMCR26 sheets. In plotting these figures, the calculated values of stiffness coefficients were referred to the longitudinal midline of each specimen and the different calculated values for each specimen and those in adjacent specimens connected using a third order polynomial smoothing function. This was done in order to give a mapping in which the values of stiffness coefficients, varied gradually over the surface of the parent SMCR26 sheets, as would be expected from the natural ordering of the composite constituent components. While the selection of a particular smoothing function imposed a specific variation between the known values that did not necessarily reflect the actual variation on the parent SMCR26 sheets, it facilitated the generation of a good 3-dimensional model that highlighted the heterogeneous nature of the parent SMCR26 sheets. The differences in distribution and magnitude of the stiffness coefficients in these two figures, was yet a further sign of the heterogeneous nature of SMCR26.

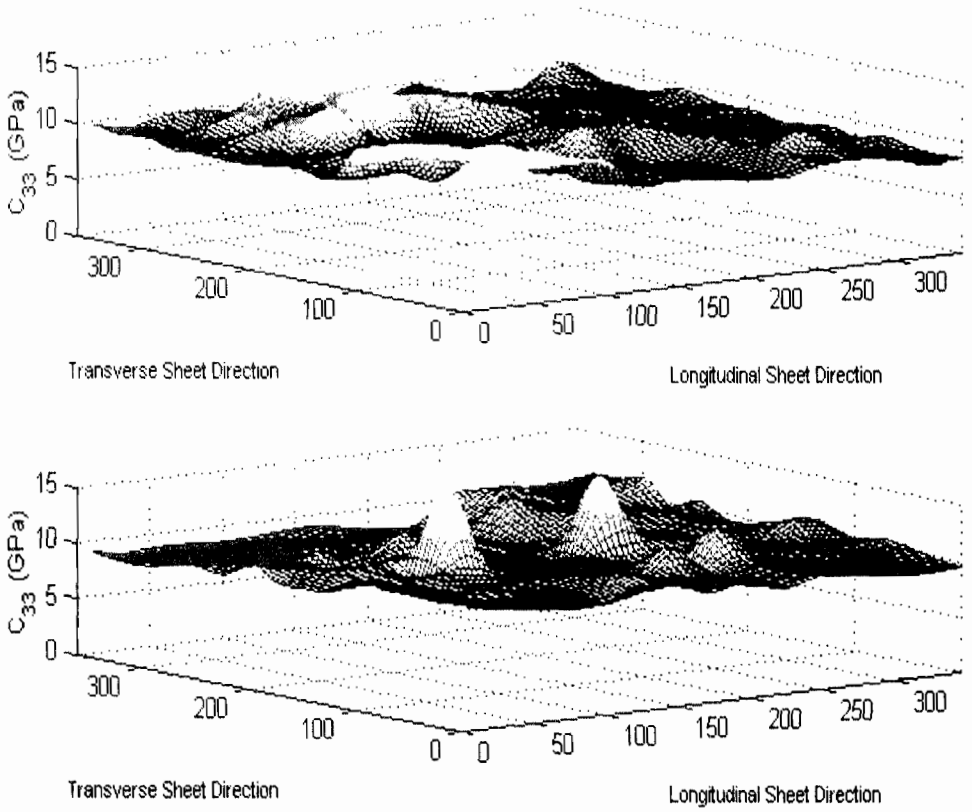

Figure 7 **Comparing the values of stiffness C_{33} for specimens that were cut with their longitudinal axis aligned parallel (a - upper) and orthogonal (b - lower) to the longitudinal direction of the SMCR26 parent sheets, based on the *zetr* correction.**

Figures 8 (a and b) show plots of the stiffness coefficients C_{33} given in Tables 5 and 6, this time based on the zero error transmission time correction (*zeal*). The small difference in magnitude between the results presented in Figures 7 (a and b) and 8 (a and b) is not all together surprising. As was stated earlier on, low velocities of transmission in SMCR26 are expected to give rise to small differences in the values of stiffness coefficients obtained from either one of the two zero error transmission time corrections (*zetr*) and (*zeal*).

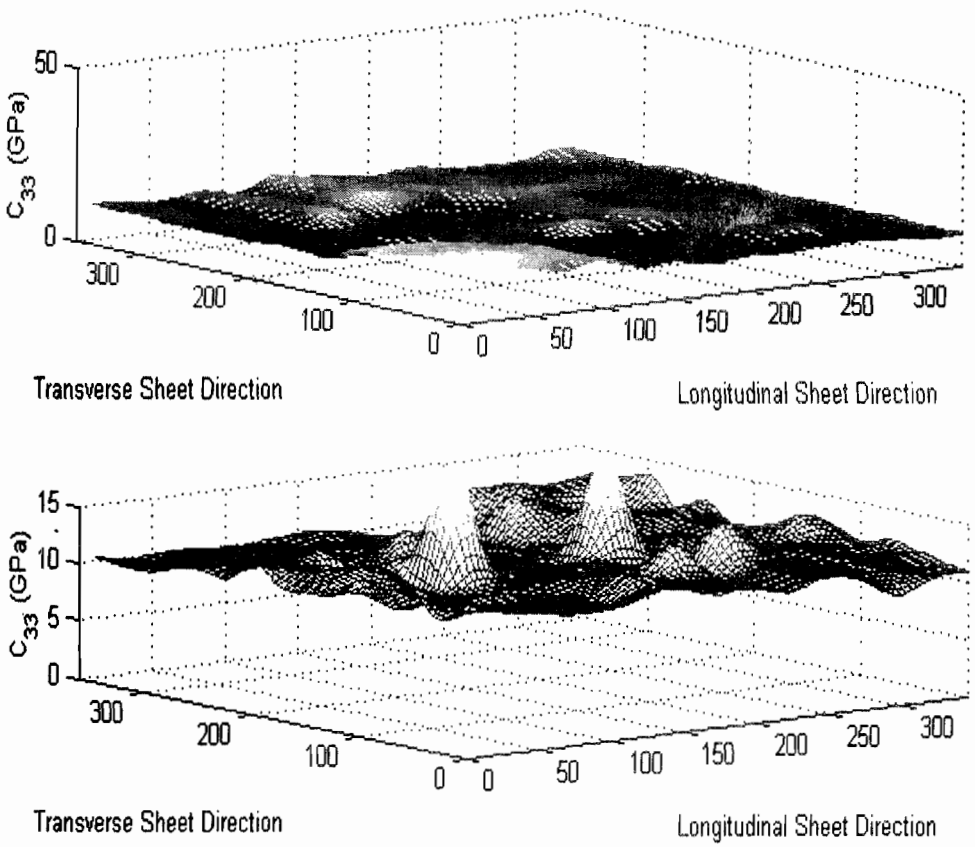

Figure 8 Comparing the values of stiffness C_{33} for specimens that were cut with their longitudinal axis aligned parallel (a - upper) to and orthogonal (b – lower) to the longitudinal direction of the SMCR26 parent sheets, based on the *zael* correction.

The SMCR26 specimens that were tested here were originally thought to be transversely isotropic, as is the case for randomly oriented short fibre reinforced composites and continuous longitudinally aligned fibre reinforced composites. The stiffness coefficients C_{22} and C_{33} are expected to be equal and so also the values of elastic modulus E_{22} and E_{33}, for transversely isotropic materials. Assuming that SMCR26 was transversely isotropic, it would be right to expect that the values of the stiffness coefficients C_{33} obtained from the through thickness ultrasonic tests, when equated to known

corresponding values of elastic modulus E_{22} obtained from the transverse vibration test, would yield values of a Poisson's ratio based parameter that is less than unity. Figures 9 and 10 show the stiffness coefficients C_{33} and elastic moduli E_{22} for specimens whose longitudinal directions were aligned parallel to and orthogonal to the longitudinal direction of the parent SMCR26 sheets. In these two figures, the lower mesh represents the stiffness coefficients C_{33}, while the upper mesh represents the elastic moduli E_{22}. The values of elastic modulus E_{22} shown in these two figures were determined using the small amplitude, transverse vibration test and have been discussed elsewhere (Maringa, 2002). The two figures show the values of the stiffness coefficients C_{33} to be smaller on average, than the values of the principal elastic moduli E_{22}, a fact that is clear from plots of the difference $(E_{yy} - C_{zz})$ shown in Figures 11 and 12. Comparison of the values of stiffness coefficients C_{33} obtained and the elastic moduli E_{22} quickly verifies whether a material is transversely isotropic or not, a point that is pursued further on in the paper.

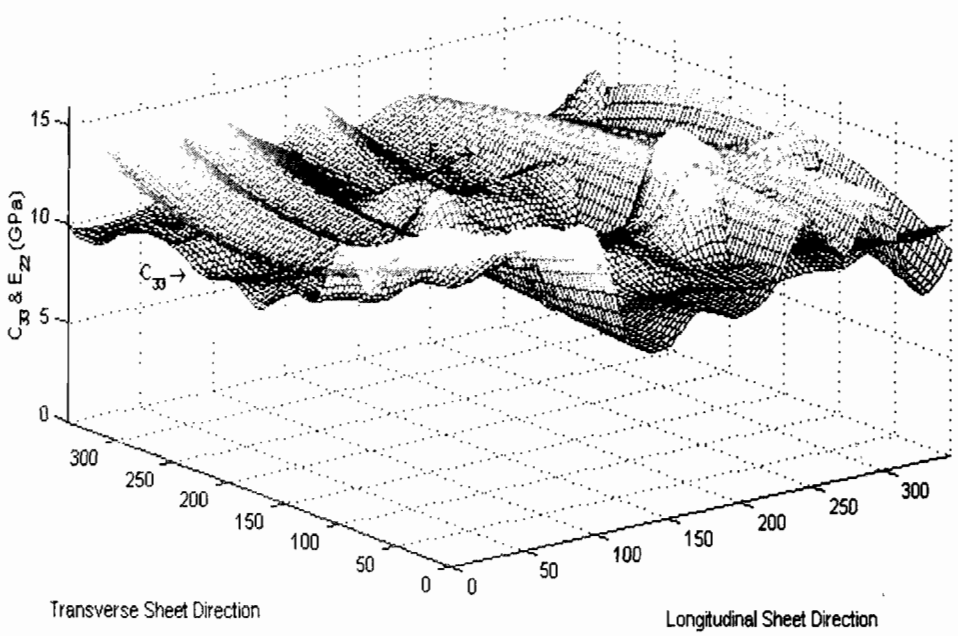

Figure 9 **Comparing the C_{33} and E_{22} values for specimens that were cut with their longitudinal axis aligned parallel to the longitudinal direction of the SMCR26 parent sheets.**

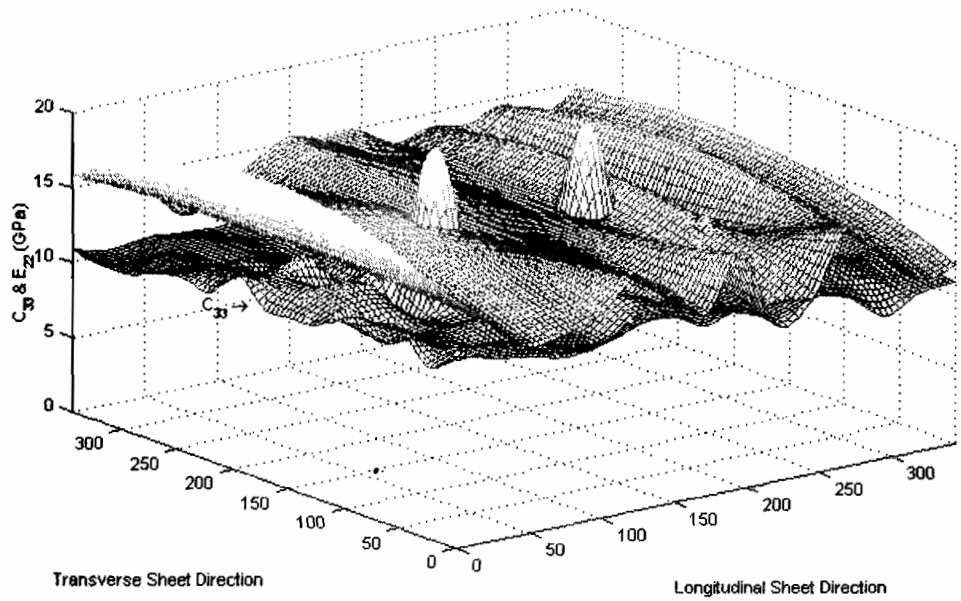

Figure 10 **Comparing the C_{33} and E_{22} values for specimens that were cut with their longitudinal axis aligned orthogonal to the longitudinal direction of the SMCR26 parent sheets.**

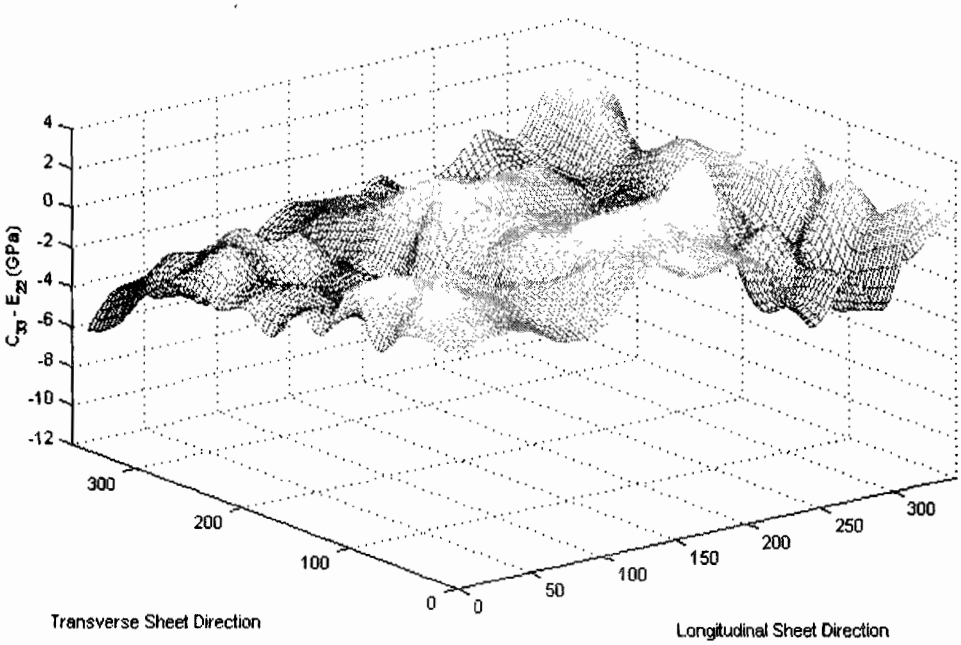

Figure 11 **The difference $(E_{yy} - C_{zz})$ for specimens that were cut with their longitudinal axis aligned parallel to the longitudinal parent SMCR26 parent sheet direction.**

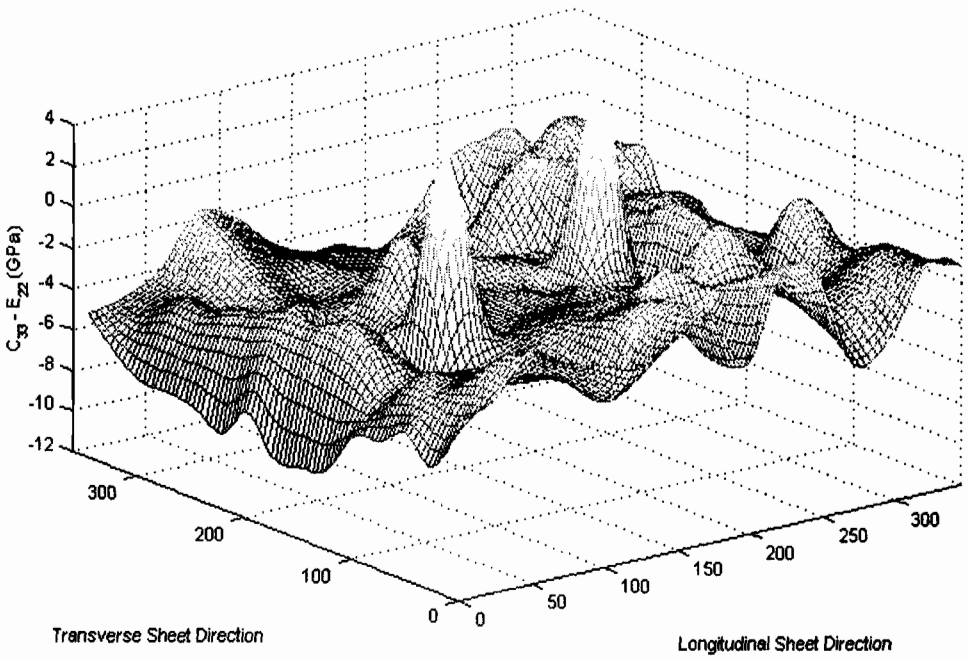

Figure 12 **The difference $(E_{yy} - C_{zz})$ for specimens that were cut with their longitudinal axis aligned orthogonal to the longitudinal parent SMCR26 parent sheet direction.**

Maringa, (2002) showed the relationship, $a = E_{22}/C_{33}$ to hold for transversely isotropic materials, where the parameter a was defined as a function of the sum of various products of the Poisson's ratios of a material. From the known fact that the absolute values of the Poisson's ratios of materials are less than unity, the parameter a must therefore, be less than unity, a condition that can only be satisfied for values of stiffness coefficient C_{33} that are greater than the elastic moduli E_{22}. Figures 11 and 12, in the present work however, show the values of the coefficient C_{33} to be less than the values of the elastic modulus E_{22}, a sign that SMCR26 is not transversely isotropic, as would be expected of it as a randomly oriented short fibre reinforced composites. The possible causes of this departure from the norm are a reinforcing fibre strand density that is lower in the through thickness plane and orientations of the reinforcing fibre strands that are not exactly transverse in the transverse in-plane direction and in the out-of-plane direction. This last effect becomes clear from a close inspection of Figure 13. The figure shows that an orientation of the reinforcing fibre strand that is not transverse gives rise to

a higher effective fibre thickness and a higher contribution of the longitudinal fibre properties to the elastic properties of the composite in the respective direction(s).

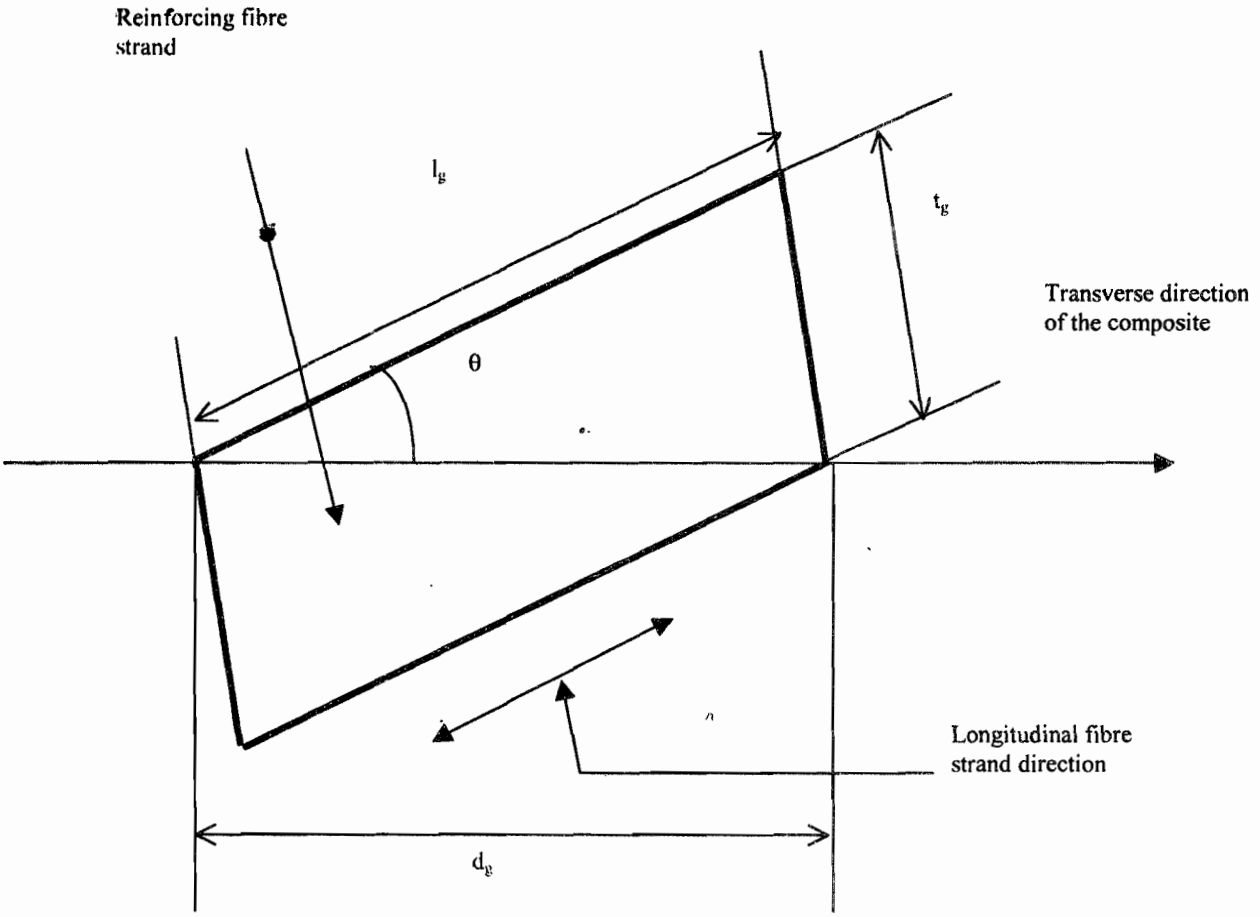

Figure 13 The effective thickness (d_g) of a re-oriented reinforcing fibre strand

The elastic modulus in such a case will be higher than the elastic modulus in the transverse direction of a composite in which the fibres are perfectly aligned. The fibre nominal length of the reinforcing glass fibre in SMCR and the nominal glass fibre strand thickness are known to be within the ranges 25 mm to 50 mm and 2.0 mm to 2.6 mm (Garroch, 1996; Loweinstein, 1972). Because the nominal diameter of the reinforcing glass fibre strands is only marginally smaller than the thickness of the SMCR26 parent sheets of 3 mm, there is very little scope for re-orientation of the fibres in the out-of-plane direction. The in-plane dimensions of the central charge area of the SMCR26

parent sheets of 345 mm × 360 mm do on the other hand give a lot of room for re-orientation. The fibre strands can in fact be re-oriented such that they are in certain cases aligned with their length fully in the "transverse" direction. The strengthening effect in the "transverse" in-plane direction will therefore be higher that in the out-of-plane direction. This is consistent with the results obtained that show the values of the stiffness coefficients C_{33} to be less than the values of the effective average elastic modulus E_{22} in the "transverse" in-plane direction. A more rigorous study of the changes in the effective thickness of the reinforcing fibre strand with their changing orientation is available in the work carried out elsewhere by Maringa (2002).

6.0 CONCLUSIONS

- Maximum, minimum, mean and standard deviation values of stiffness coefficients of 21.03 GPa, 9.35 GPa, 11.52 GPa and 1.23 GPa, as well as 16.31 GPa, 8.96 GPa, 11.41 GPa and 1.53 GPa were obtained for specimens with their longitudinal axes oriented in the longitudinal and transverse SMCR26 parent sheet directions, respectively.
- The manner in which the values of through thickness stiffness coefficients determined in the present work varied over the surface of the parent SMCR26 sheets clearly showed them to be heterogeneous.
- Though SMCR, like other randomly oriented short fibre reinforced composites, is expected to be transversely isotropic, the results obtained here indicated otherwise.

Clearly, therefore, the aims set out at the onset of the project, those of determining the magnitude, as well as the directional and spatial dependency of the through thickness values of stiffness coefficients were achieved.

ACKNOWLEDGEMENTS

Dr. S. O. Oyadiji, Mike Amprikidis, George Georgiadis, Paul Townsend and the late Mike Tillotson, all of the school of Engineering at the University of Manchester, UK, for their assistance in different ways, in the course of undertaking the experimental work reported here.

REFERENCES

Birley A. W. (1992) *Polymer Sheet: Manufacture and Applications*, in *Concise Encyclopaedia of Polymer Processing and Applications*, edited by Corish P. J., pp. 514 – 517, Pergamon Press, Oxford.

Bowen D. H., (1992) *Composites: Manufacturing Overview*, in *Concise Encyclopaedia of Polymer Processing and Application*", edited by Corish P. J., pp. 132 - 143, Pergamon Press, Oxford.

Lonsdale C. P. and Meyer P. A., (March 29, 2000) Use of Phased Arrays for Ultrasonic Testing of Railroad Wheels, *American Society for Non-destructive Testing Ninth Annual Research Symposium*, Birmingham.

Hackenberger D. and Rose J. L., (Spring and Summer 1998) Emerging Technology – Guided Wave Ultrasonics, *Technical Features, ND Times*, **2** (2), http://www.krautkramer.com/company_publications/nd_times/Spring_98.pdf.

Frielinghaus R., (2001) Examples of Ultrasonic Applications for Non-destructive Testing of Plastics, *Krautkramer*, GmbH and Co. Hurth, Germany, http://www.krautkramer.com/reference/intro.htm.

Garroch C. (1996) *Thermoelastic Assessment of Moulded Fibre Reinforced Composites*, Ph.D. Thesis, University Of Manchester.

Gibson R. F (1994) *Principles of Composite Material Mechanics*, 1994, McGraw-Hill International Edition.

Halmshaw R. R., (1991) *Non-destructive Testing*, 2nd ed., Edward Arnold, London.

Hinsley J. F., (1959), *Physical acoustics - Principles and Methods*, McDonald and Evans Ltd, London.

Hull D. and Clythe T. W., (1996) *An Introduction to Composite Materials*, Cambridge University Press.

Hull B. and John V., (1988) *Non-Destructive Testing*, Macmillan Education Limited, Hong Kong.

Johnson A. F. (3, July 1986) Comparison of the Mechanical Properties of SMC With Laminated GRP Materials, *Composites*, **17**, 233 - 239.

Johnson A. F. (1992) Glass-reinforced Plastics: Thermosetting Resins, in, Concise Encyclopaedia of Polymer Processing And Applications, edited by Corish P. J., pp. 331 – 337, Pergamon Press, Oxford.

Kavishe F. P. L., (1997) Basic Principles of Ultrasonic Testing, Nairobi University Press, Nairobi.

Khoury M., Tourtollet G. E. and Schroder A., (1999) The Contactless Measurement of the Elastic Young's Modulus of Paper by an Ultrasonic Technique, *Ultrasonics* **37**, 133 – 139.

Kirkwood W. F., Feng W.W, Scott R. G., Stret R. D., Goldberg A., (1985) *Mechanical Properties and Science of Engineering Materials*, in *A Handbook of Mechanics, Materials and Structures*, Alexandre B. (Editor), John Wiley and Sons.

KrautKrämer J., KrautKrämer H., Grabendörfer W., Gregor M, Niklas L., Frielinghaus R., Kaule W., Schlemm H., Schlengerman U. and Steiger H., (1990) *Ultrasonic Testing of Materials*, 4th edition, Springer-Verlag, Berlin.

Loeweinstein K. L., (1973) Manufacturing Technology of Continuous Glass Fibres, Elsevier Scientific Publishing Company.

Maringa M., (2002) Investigating the Mechanical Properties of Sheet Moulding Compound (SMCR26), Detecting Fatigue Damage and Monitoring Fatigue Damage Accumulation in the Material, Ph.D. Thesis, University of Manchester, UK.

Melby E. G. and Castro J. M. (1989) Glass - Reinforced Thermosetting Polyester Moulding: Materials and Processing, in Comprehensive Polymer Science. The Synthesis, Characterisation, Reactions and Applications of Polymers, **7**. Specialty Polymers and Polymers Processing, pp 51 - 109, Pergamon Press, Oxford.

Michael Berke, (2001) Non-destructive Material testing with Ultrasonics - Introduction to the basic Principles, Krautkramer, GmbH and Co. Hurth, http://www.krautkramer.com/reference/intro.html.

Rose J. L., Pilarski A. and Huang Y., (1990) Surface Wave Utility in Composite Material Characterisation, *Journal of Nondestructive Evaluation* **1**, 247 – 265.

Rose J. L., Ditri J. J., Huang Y., Dandekar D. P. and Chou S-C, (1991) One-Sided Ultrasonic Inspection Technique for the Elastic Constant Determination of

Advanced Anisotropic Materials, *Journal of Nondestructive Evaluation*, **10** (4), 159 – 166.

Rose J. L., (1999) *Ultrasonic Waves in Solid Media*, Cambridge University Press.

Shutilov A. V., (1988) *Fundamental Physics of Ultrasound*, Gordon Breach Science Publishers, New York.

Splitt G., (2001) Piezocomposite Transducers – a Milestone for Ultrasonic Testing, *Krautkramer*, 2001, GmbH and Co. Hurth, Germany, http://www.krautkramer.com/reference/intro.htm.

Standards Steel (2001) Phased Array Systems, *Krautkramer*, http://www.krautkramer.com/arrayweb.

Stumpf F. B., (1980) *Analytical Acoustics*, Ann Arbor Science.

Van Buskirk W. C., Cowin S. C. and Carter Jr. R., (1986) A Theory of Acoustic Measurement of the Elastic Constants of a General Anisotropic Solid, *Journal of Material Science*, **21**, 2759 – 2762.

Whelan T. and Goff J. (Nov. 1986) Sheet Moulding Compound (SMC), *British Plastics and Rubber*, (24).